Numerical Simulation of Consolidation Settlement of Pervious Concrete Pile Composite Foundation under Road Embankment

Jiong Zhang, Ph.D.[1]; Xinzhuang Cui[2]; Dan Huang[3]; Qing Jin[4]; Junjie Lou[5]; and Weize Tang[6]

Abstract: Having the advantages of high permeability and high strength, pervious concrete is suitable for improving ground-bearing capacity. In the Yellow River Delta, a pervious concrete pile (PCP) composite foundation has been constructed to reduce settlement of an expressway embankment. To study the working mechanism of PCPs, a numerical model was constructed based on the finite-difference method and Biot's consolidation theory, which was validated by data from in situ tests. The excess pore-water pressure, pile–soil stress ratio, lateral displacement, and settlement of the PCP composite foundation under the loading of the road embankment were numerically calculated and compared with those of gravel pile and low-grade concrete pile composite foundations. Comparisons show that the dissipation of excess pore-water pressure in the PCP composite foundation was fastest, which implied that PCPs can significantly mitigate the development of excess pore-water pressure and thus enhance subsoil strength. Furthermore, the PCP composite foundation showed minimal postconstruction settlement and lateral displacement. Therefore, PCP is particularly suitable for reinforcing subsoil that has low strength and poor permeability. **DOI: 10.1061/(ASCE)GM.1943-5622.0000542.**

Author keywords: Pervious concrete pile; Composite foundation; Excess pore-water pressure; Settlement.

Introduction

The Yellow River Delta of China is formed by sediments deposited at the mouth of the river; alluvial silt is thus widely distributed in the Yellow River Delta and has unique characteristics, such as a low liquid limit and plasticity index, low cohesion, low strength, intensive capillarity, narrow size distribution, and poor water stability. Expressways will soon be built in the Yellow River Delta because of the economic development in the area. In other projects, composite foundation technology has been widely used to reduce excessive settlement of underconsolidated subsoil caused by subgrade weight. In this paper, the pavement is a composite structure with a surface course, base, and subbase; the embankment is a compacted soil layer below the subbase of a road; and the term subgrade includes all layers above the natural ground surface. The term subsoil refers to the natural soil below a road embankment, which can be divided into two zones: the reinforced zone and the substratum, which is under the reinforced zone.

[1]Lecturer, School of Civil Engineering, Shandong Univ., Jinan 250061, P.R. China. E-mail: jiongzhang@sdu.edu.cn

[2]Professor, School of Civil Engineering, Shandong Univ., Jinan 250061, P.R. China (corresponding author). E-mail: cuixz@sdu.edu.cn

[3]Graduate Student, School of Civil Engineering, Shandong Univ., Jinan 250061, P.R. China. E-mail: huangdantf@163.com

[4]Lecturer, School of Civil Engineering, Shandong Univ., Jinan 250061, P.R. China. E-mail: jinqing@sdu.edu.cn

[5]Graduate Student, School of Civil Engineering, Shandong Univ., Jinan 250061, P.R. China. E-mail: lou_jj@126.com

[6]Graduate Student, School of Civil Engineering, Shandong Univ., Jinan 250061, P.R. China. E-mail: 809775169@qq.com

Note. This manuscript was submitted on May 18, 2014; approved on May 5, 2015; published online on September 14, 2015. Discussion period open until February 14, 2016; separate discussions must be submitted for individual papers. This paper is part of the ***International Journal of Geomechanics***, © ASCE, ISSN 1532-3641.

In recent years, composite foundation technology has made significant advances and has been used to enhance ground-bearing capacity and reduce settlement and liquefaction potential of ground (Ariyarathne et al. 2013; Haldar and Babu 2010; Yao et al. 2015). A vertical reinforcement composite foundation may be divided into granular piles, flexible piles, and rigid piles. For example, sand piles and gravel piles (GPs) are granular piles, cement–soil piles are flexible piles, and both cement fly-ash gravel (CFG) piles and low-grade concrete piles (LCPs) are rigid piles.

Granular piles have been widely used in engineering because they can accelerate the rate of consolidation and reduce the liquefaction potential of sand or silty soil (Hughes and Withers 1974; Lee and Pande 1998; Ferreira Pinto and Delgado Rodrigues 2008; Poorooshasb and Meyerhof 1997). However, the stiffness and strength of granular piles are low and depend on the confining pressure of the surrounding soil (Guetif et al. 2007). When a granular pile is applied to soft clay, organic soil, and peat soil, the shallow granular pile is prone to expansion failure, so the bearing capacity of the ground is improved only marginally, and settlement after construction cannot be effectively mitigated. In contrast, rigid piles such as LCPs and CFG piles can overcome the weak bonding problem of granular piles (Sariosseiri and Muhunthan 2009; Le Hello and Villard 2009; Zheng et al. 2008; Jia et al. 2011; Ge et al. 2015). Jia et al. (2011) analyzed the CFG pile composite foundation with field tests combined with a numerical simulation method and found that CFG can significantly improve ground-bearing capacity. However, rigid piles typically have poor permeability and slow the consolidation of a foundation. A substantial amount of research has been conducted on multi-pile composite foundations with pervious piles. For instance, Chen et al. (2004) performed field tests on CFG-lime multi-pile composite foundations. Zheng et al. (2008) used the finite-element method to study CFG-lime pile composite foundations and proved that settlements of this type of composite foundation can be mitigated; however, the construction process of multi-pile composite foundations is not uniform, making it difficult to guarantee construction quality.

Recently, an innovative ground improvement method using pervious concrete piles (PCPs) was proposed by Suleiman et al. (2011). Pervious concrete, also referred to as porous concrete, is a mixture of Portland cement, gap-graded aggregate, and water with or without a small amount of fine aggregate. There are a large number of breakthrough pores within the aggregate skeleton. Generally, the porosity of pervious concrete is between 15 and 25%, and the permeability is typically between 2 and 6 mm/s but can be as high as 10 mm/s (Tennis et al. 2004; Montes et al. 2005; Luck et al. 2006; Kevern 2015). With high permeability, pervious concrete can also provide a compressive strength between 3.5 and 28 MPa (Schlüter and Jefferies 2002). PCPs typically have fast drainage with a high bearing capacity; thus, PCPs share the advantages of both flexible and rigid piles. Cui et al. (2012) studied the dynamic characteristics of PCP composite foundations under earthquake loads and found that PCPs have a significant damping effect and pressure-reduction effect. The excess pore-water pressure induced by an earthquake was dissipated quickly, and foundation liquefaction was effectively inhibited.

A PCP is similar to sand and granular piles. Therefore, the consolidation theories for sand and granular pile composite foundations can be referenced to a certain degree to study the consolidation of PCP composite foundations. Barron (1948) proposed an axisymmetric model to investigate the radial consolidation for vertical sand piles. This solution has been extended to reflect more complex and realistic conditions in later studies. Yoshikuni (1979) proposed the concept of stress concentration for foundations reinforced by granular columns. As then, this concept has been used in nearly all consolidation theories for composite foundations. Majorana et al. (1983) established a finite-element equation of consolidation that considered complex factors and used it to analyze a gravel column foundation of tanks. Zhu and Yin (2004) and Leo (2004) analyzed this problem in a coupled horizontal–vertical fashion. On the basis of this coupled analysis method, studies presented by Conte and Troncone (2009) considered the time-dependent effects of external loads. Xie et al. (2009) developed a general solution for computing the consolidation rate of a composite foundation reinforced with columns by considering the variation of the horizontal permeability coefficient of the disturbed soil, changes in the total average stress with depth, and the time effects of construction. However, all work mentioned previously focused on rigid loading, and the theories were based on the assumption of the equal strain condition (i.e., the soil and vertical drain have an equal strain at any depth). This assumption is not suitable for analyses of embankment consolidation. Embankment loading is a flexible load, and thus the deformations of the soil and piles are uncoordinated (Subba Rao et al. 2002), particularly in rigid pervious piles (i.e., PCPs). However, little research has been conducted on the consolidation and settlement of PCP composite foundations.

To reduce the settlement of subsoil composed of alluvial silt in the Yellow River Delta, traditional piles such as LCPs and GPs are used in engineering applications. However, many investigations have shown that postconstruction settlements of embankment remain large. In this study, a composite foundation was constructed with a group of PCPs at a test site of the Jinan-Dongying Expressway. On the basis of the finite-difference method and Biot's consolidation theory (Biot 1962), the behaviors of PCP composite foundations subjected to embankment loading are numerically simulated. Comparisons are performed with results from in situ tests to validate the numerical method; comparisons are also made with GP and LCP composite foundations to further explain the advantages of PCP composite foundations.

In Situ Tests

The test site is located in a construction section of the Jinan-Dongying Expressway, which is one of the key national highways of China. To determine the physical and mechanical parameters of silty subsoil, a gravel cushion, and embankment soil, a series of laboratory geomechanical tests, including a triaxial shear test and a permeability test, were performed according to the Chinese Technical Code for Ground Treatment of Buildings JGJ 79-2002 (MCPRC 2002) and the Technical Specification for Construction of Highway Subgrades JTG F10-2006 (MTPRC 2006). The parameters are shown in Table 1.

The groundwater level was measured to be 0.5 m below ground. A group of PCPs was installed in a square arrangement to form a composite foundation. The mix proportions of the pervious concrete used are shown in Table 2. The spacing between the piles was 2.4 m, the pile diameter was 0.6 m, and the pile length was 10 m. An installation system using a vibrating immersed tube was used to install PCPs. The installation system consists of a steel tube with a flapper valve at the tip. During pipe advancement, the tip of the flapper valve was closed. Once the desired depth was reached, the pervious concrete was placed from the top of the pipe, and the pipe was lifted upward, and the tip of the cone started to open.

A gravel cushion with a thickness of 0.5 m was paved above the subsoil. The dimensions of the subgrade were determined by the Chinese Specifications for Design of Highway Subgrades JTG D30-2004 (MTPRC 2004). A sketch of a portion of the composite foundation and subgrade is presented in Fig. 1. During construction, the variation of the embankment height with time was recorded and is shown in Fig. 2.

Table 2. Mix Proportions of PCPs

Materials/Property	Value
Target porosity (%)	15
W/C	0.36
Cement (kg/m^3)	335
Water (kg/m^3)	121
Aggregate (5–10 mm) (kg/m^3)	1,622
Water reducer dosage (%)	0.80

Table 1. Physical and Mechanical Parameters of Subsoil and Embankment Soil

Material	Density (kg/m^3)	Cohesion (kPa)	Internal friction angle (degrees)	Elastic modulus (kPa)	Poisson's ratio	Permeability (m/s)	Void ratio
Silty subsoil	1,980	28	17.8	5,000	0.30	1.22×10^{-8}	0.709
Gravel cushion	2,240	—	—	64,000	0.25	0.74	0.630
Embankment soil	1,870	29.3	36.5	20,000	0.40	—	—

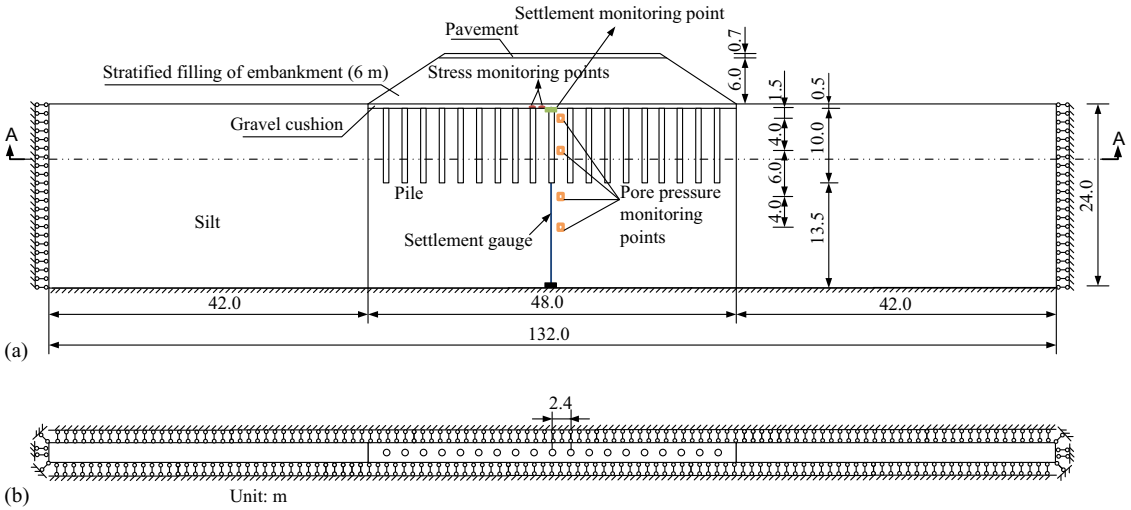

Fig. 1. Cross section of the composite foundation and road embankment geometric model: (a) cross section; (b) Section A-A

Arrangement of Sensors

Four pore-pressure sensors were installed underground to measure excess pore pressure at depths of 1.5, 5.5, 11.5, and 15.5 m from the ground surface. To monitor subsoil settlement, one settlement gauge was arranged at the road center of the test section, as shown in Fig. 1.

Coupled Fluid–Mechanical Interaction Model

In this study, the soil can be regarded as an equivalent continuum. Fluid transport is described by Darcy's law and also obeys Biot's theory (Biot 1962). The fluid–mechanical coupling calculation is well described by the following equations (Itasca Consulting Group 2006).

Governing Differential Equations

Mass Balance Laws

For small deformations, the fluid mass balance can be expressed as

$$-q_{i,i} + q_v = \frac{\partial \zeta}{\partial t} \tag{1}$$

where q_i = specific discharge vector; q_v = volumetric fluid source intensity; and ζ = variation of the fluid content or variation of the fluid volume per unit volume of porous material due to diffusive fluid mass transport, as introduced by Biot (1956).

For saturated fluid flow, the following equation is used:

$$\frac{\partial \zeta}{\partial t} = \frac{1}{M}\frac{\partial p}{\partial t} + \alpha \frac{\partial \varepsilon}{\partial t} - \beta \frac{\partial T}{\partial t} \tag{2}$$

where M = Biot modulus; p = pore pressure; α = Biot coefficient; ε = mechanical volumetric strains; T = temperature; and β = undrained thermal coefficient, which accounts for the fluid and grain thermal expansions. This study does not consider the thermal expansion effect, so Eq. (2) can be simplified as

$$\frac{\partial \zeta}{\partial t} = \frac{1}{M}\frac{\partial p}{\partial t} + \alpha \frac{\partial \varepsilon}{\partial t} \tag{3}$$

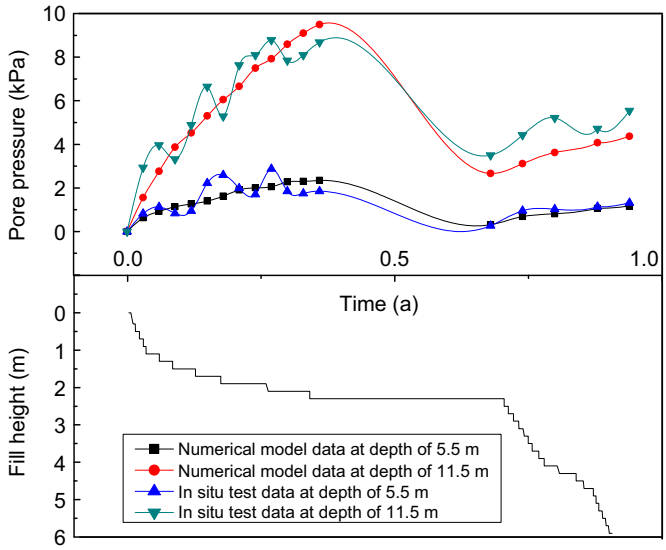

Fig. 2. Comparison of time history of excess pore-water pressure in a composite foundation

Fluid Transport (Darcy's Law)

Fluid transport is described by Darcy's law. For a homogeneous, isotropic solid and constant fluid density, this law is given in the form

$$q_i = -k(p - \rho_f x_j g_j)_{,i} \tag{4}$$

where k = intrinsic permeability of porous medium; ρ_f = fluid density; and g_i where $i = 1$, 2, and 3 are the three components of the gravity vector.

Constitutive Laws

The variation of fluid content is related to the change in pore pressure; conversely, changes in pore pressure will lead to changes in fluid content. The constitutive response for the porous solid has the form

$$\Delta\sigma_{ij} + \alpha \Delta p \delta_{ij} = H^*_{ij}(\sigma_{ij}\Delta\varepsilon_{ij} - \Delta\varepsilon^T_{ij}) \tag{5}$$

where $\Delta\sigma_{ij}$ = stress rate; δ_{ij} = Kronecker delta; H^*_{ij} = functional form of the constitutive law; ε_{ij} = strain rate; and ε^T_{ij} = thermal strain rates.

Compatibility Equation

The relation between the strain rate and the velocity gradient is

$$\varepsilon_{ij} = (v_{i,j} + v_{j,i})/2 \tag{6}$$

where v = velocity of the porous solid.

All equations described above can be modeled with a fast Lagrangian analysis of continua, *FLAC* (Itasca Consulting Group 2006). In *FLAC-3D*, fluid–mechanical coupling uses continuum theory; solids and fluids are regarded as overlapping continuums, and the properties of continuous media in the system, including porous media and fluids, can be described by continuous variables. These imply that the governing equations of fluid–mechanical coupling can be built for a specific physical phenomenon and that the fluid–mechanical coupling can be reflected by the governing equations.

Geometric Model

The geometric model used in the numerical simulation has been determined based on the in situ test data. One basic unit of the composite foundation, which is composed of 19 round piles, is selected for mechanical analyses, as shown in Fig. 1. The arrangement parameters in each case, which include the spacing between piles, the pile diameters, and the pile lengths, are set equal to those used in the field tests. Piles and their surrounding soil have been closely connected (i.e., glued together). At the pile–soil interface, nodes are shared by both pile and soil, and the displacements are continuous.

Mechanical Parameters and Material Model

The physical and mechanical parameters of the subsoil, gravel cushion, and embankment soil used in the numerical simulation are obtained from laboratory geomechanical tests, as shown in Table 1. The consolidation settlements of four different kinds of foundations have been compared, including a natural foundation, a GP composite foundation, a LCP composite foundation, and a PCP composite foundation. The mechanical parameters of three types of piles are shown in Table 3. A Mohr–Coulomb material is used for the subsoil and embankment soil, and an elastic model is adopted for piles.

Boundary Conditions

During the calculation, the bottom boundary of the 3D model is fixed in all directions, whereas the front, back, left, and right boundaries are fixed in the normal direction, as shown in Fig. 1. The left, right, and bottom boundaries are considered impermeable. The pore pressures are set to zero above the ground-water level.

Validation of the Numerical Model

To validate the numerical simulation method, the numerical results were compared with the in situ test results. The actual stratified filling process was simulated according to the variation in the embankment height with time, as shown in Fig. 2. Time histories of the excess pore pressure and settlement throughout one year of construction were monitored in situ and compared with numerical results in Figs. 2 and 3, respectively. In Fig. 2, the calculated excess pore-water pressures at depths of 5.5 and 11.5 m from the surface are similar to the in situ measurements. The fluctuations of the former data are large because the underground water level changes with the change of seasons, fluctuating approximately 0.5 m below ground. The later portions of the pore pressure do not agree at a depth of 11.5 m. This may be because actual pores in the subsoil become smaller as embankment loads increase, causing permeability to decrease. However, the permeability remains unchanged in the simulations, which finally show the calculated pore pressure becoming smaller than that in field tests, as shown in Fig. 2.

Fig. 3 compares the settlement calculated by the numerical model and the data measured in situ. As shown in Fig. 3, the settlements acquired from the numerical simulation are similar to the measured data from the in situ tests when the thickness of embankment was less than 2 m. However, if the thickness of embankment was larger than 2 m, a significant difference appears and increases with the thickness of the embankment. This is likely because the settlement relates to the elastic modulus of the substratum. As the thickness of the embankment increases, which represents the stress level experienced by the foundation, the elastic modulus decreases, whereas the initial modulus measured by the laboratory test is used in the numerical simulation; thus, the higher the embankment is filled, the greater the difference between the embankment settlement obtained by the numerical simulation and the measurements in situ. Another reason for this discrepancy is that the strength of PCPs constructed in situ is typically weaker than

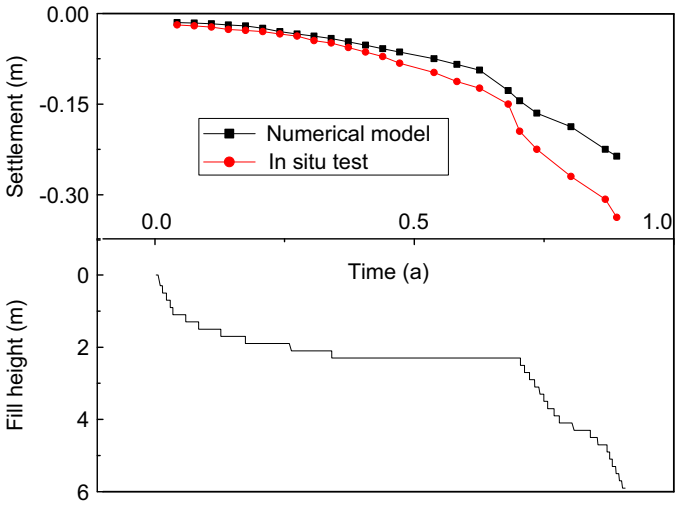

Fig. 3. Comparison of time history of settlement

Table 3. Mechanical Parameters of Piles

Types of pile	Elastic modulus (MPa)	Poisson's ratio	Specific weight (kg/m^3)	Permeability (m/s)	Porosity
LCP	12,000	0.2	2,040	1.02×10^{-10}	0.100
GP	200	0.3	2,240	7.14×10^{-3}	0.176
PCP	12,000	0.2	2,040	7.14×10^{-3}	0.176

that of specimens prepared in a laboratory. However, the trends of the calculated and measured settlements are similar.

In general, when the embankment height is relatively large, differences between the calculated and measured excess pore pressure and settlement are greater, but the trends of these variables are found to be similar; therefore, the numerical simulation method is reliable to a certain extent.

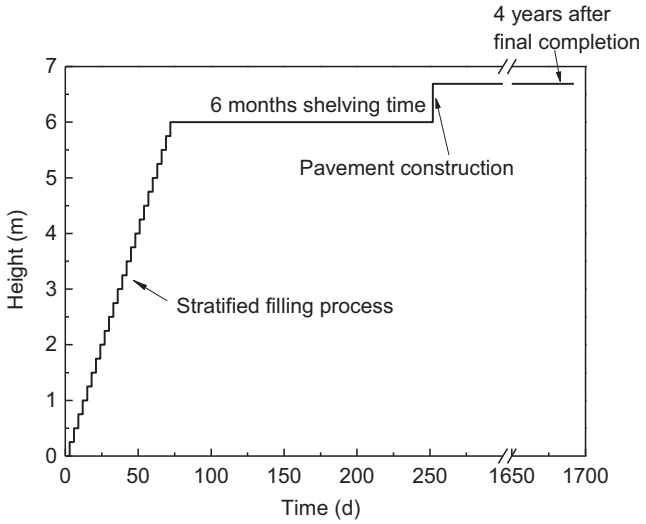

Fig. 4. Ideal variation of embankment loads with time for numerical calculation

Numerical Results and Analyses

On the basis of the real construction procedure, an ideal variation of embankment loads with time in the calculations is determined, as shown in Fig. 4. Stratified filling is used, and the thickness of each compacted layer is 25 cm. According to the Chinese Specifications for Design of Highway Subgrades JTG D30-2004 (MTPRC 2004), pavement must be constructed at least six months after completion of the embankment construction. Because pavement construction is fast, pavement loading is exerted on the embankment in one step. Once the first layer of the embankment soil is paved, the calculation of consolidation should be started to compare a natural foundation with three different composite foundations.

Pore Pressure

Fig. 5 shows the variations of excess pore-water pressure in the composite foundation with time. Pore pressure is captured beneath the centerline of the embankment. During the loading process, a large excess pore-water pressure is generated in the silty subsoil and then dissipated gradually. As Fig. 5 shows, compared with the natural foundation and the LCP composite foundation, the pore pressures of the GP composite foundation and the PCP composite

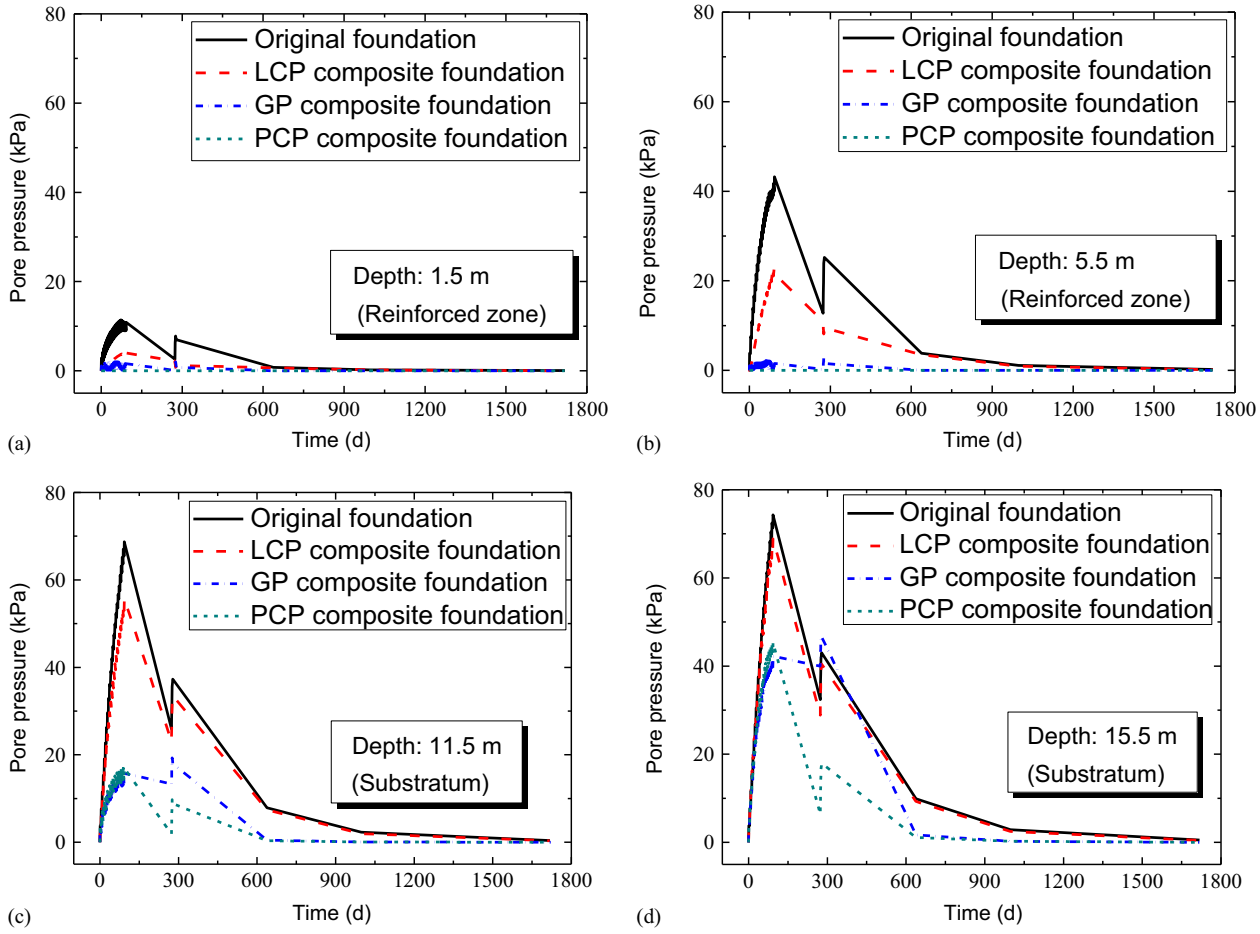

Fig. 5. Variations of excess pore-water pressure in composite foundation with time: (a) depth = 1.5 m; (b) depth = 5.5 m; (c) depth = 11.5 m; (d) depth = 15.5 m

foundation are smaller during stratified filling. This is true because the permeability of LCPs is small, preventing the pore pressure from dissipating in such a short time, thus resulting in high pore pressure. The pore pressure of the LCP composite foundation is still much greater than that of the GP and PCP composite foundations after a six-month waiting period. Compared with the GP foundation, the excess pore-water pressure in the PCP foundation is small because PCPs have a higher stiffness, which results in a smaller soil-volume deformation and thus a smaller pore pressure.

In general, pore pressure increases with depth. However, there are different distribution modes along the depth for different foundations, as shown in Fig. 6. For the original foundation, the increase rate of pore pressure along with depth becomes increasingly slow, and the distribution mode of pore pressure is very similar to the solution of Terzaghi's one-dimensional consolidation equation for homogeneity soil (Terzaghi 1925). Although for pervious pile (e.g., PCP and GP) composite foundations, the increase rate of pore pressure along with depth becomes increasingly fast because the drainage paths change at different depths for a PCP foundation. Within the reinforced zone, the drainage paths are primarily horizontal, whereas in the substratum, the drainage paths are primarily vertical and are much longer. For LCP composite foundations, the stiffness of the whole foundation is increased, but the drainage type is not changed compared with original foundation; thus, the distribution mode of pore pressure with depth falls in between the previously mentioned modes.

Pile–Soil Stress Ratio

The pile–soil stress ratio is the vertical stress ratio of the top of the piles and the center of the subsoil surface between piles, which indicates the ratio of the stress born by the piles and soil, respectively (as shown in Fig. 7). Fig. 8 shows the variations of the pile–soil stress ratio with time. In the construction of the embankment, the pile–soil stress ratio shows a linear increase with time but falls slightly during the six-month waiting period. Then, the ratio stabilized after the pavement construction was finished. For PCPs and LCPs, the ratio reaches up to more than 40 at the end of the stratified filling period, which indicates that the stress concentration occurs at the top of the pile, and the piles bear most of the embankment loads.

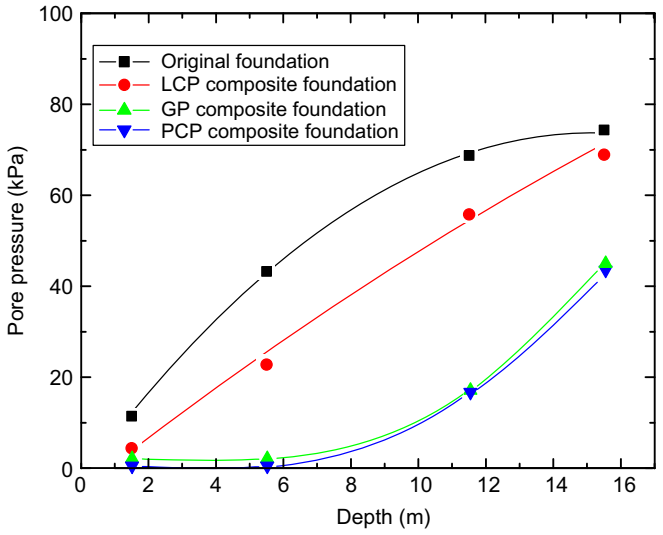

Fig. 6. Variations of excess pore-water pressure in composite foundation with depth after stratified filling process

This is true because the elastic modulus of silty subsoil is 5 MPa, which is much lower than that of PCPs and LCPs. During the waiting period, with the dissipation of excess pore-water pressure and the consolidation of subsoil, the strength of the subsoil increases, and thus the pile–soil stress ratio decreases. Compared with PCPs and LCPs, the pile–soil stress ratio of GPs is much smaller. This is because GPs have a lower stiffness than PCPs and LCPs. For soft subsoil, a large pile–soil stress ratio is required, which indicates that the piles can bear most of the upper loads and provide sufficient bearing capacity to meet engineering requirements.

Lateral Displacement of the Foundation Surface

Fig. 9 shows the distribution curves of the foundation surface lateral displacement at different periods; the curves appear as inverted *S*-curves. The lateral displacement is generally increasing from the center of the embankment, with the largest displacement located approximately 40 m away from the centerline. The foundation surface lateral displacement gradually increases during the construction process, reaches a maximum at the time of completion, and subsequently reduces with consolidation. Additionally, as shown in Fig. 9, compared with LCPs and PCPs, GPs have a lower strength, which results in a large lateral displacement. The surface lateral displacement of the PCP foundation is effectively reduced because of its high stiffness and permeability.

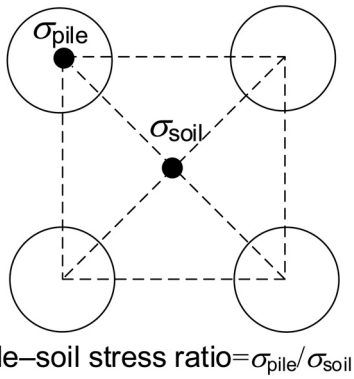

Fig. 7. Sketch of the pile–soil stress ratio

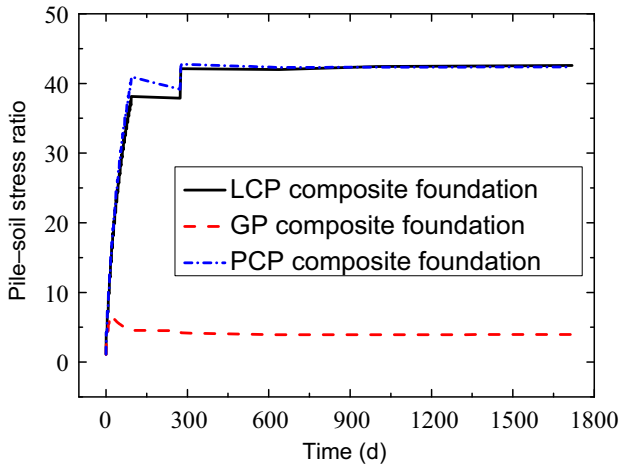

Fig. 8. Variations of the pile–soil stress ratio with time

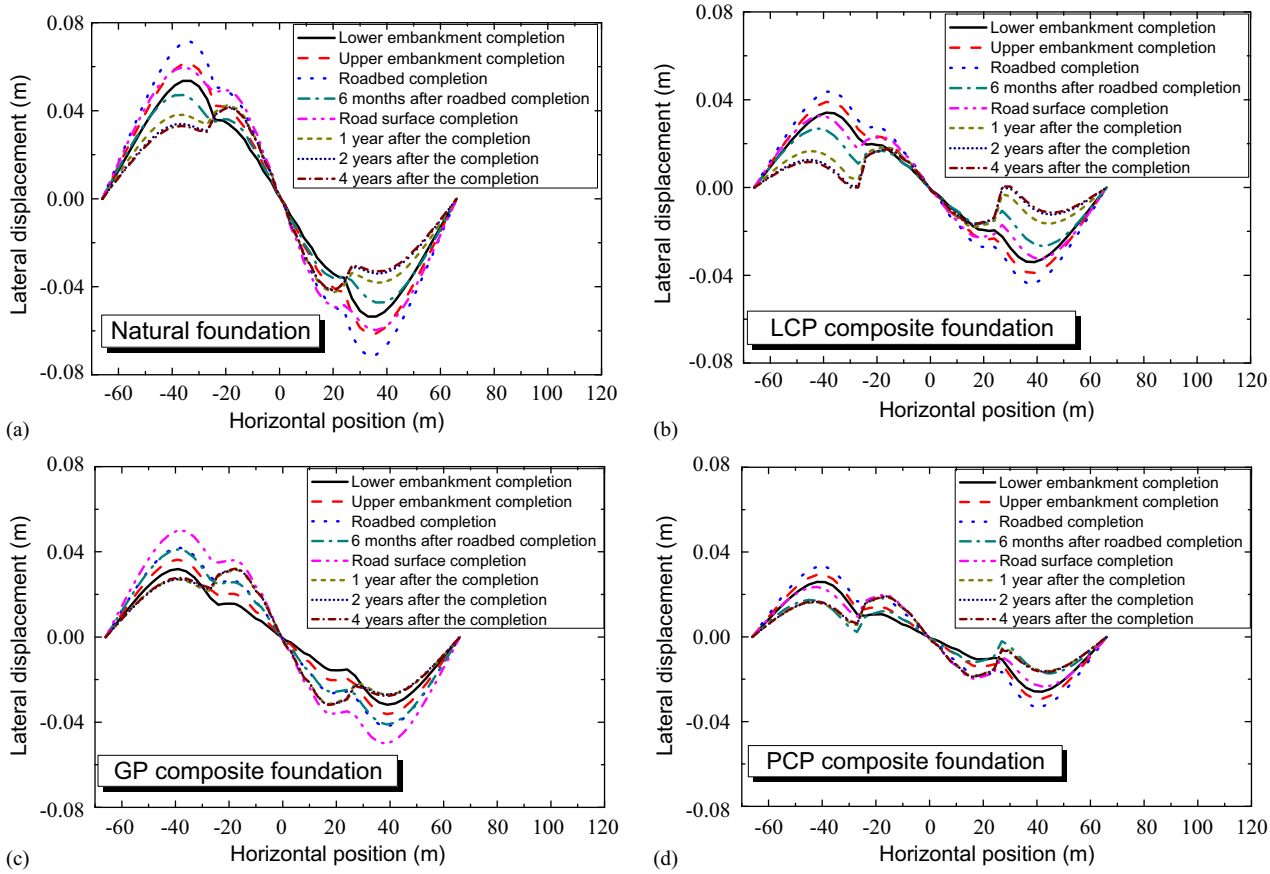

Fig. 9. Distribution curves of ground surface lateral displacement at different periods: (a) natural foundation; (b) LCP composite foundation; (c) GP composite foundation; (d) PCP composite foundation

Settlement

In this study, total settlement and postconstruction settlement of the foundations were both investigated. Total settlement includes settlement during construction and postconstruction settlement. However, postconstruction settlement is the most important factor in engineering because it can have harmful effects on the road embankment and adversely affect road operations.

Foundation Surface Settlement

Distribution curves of the total settlement of the foundation surfaces during different periods are shown in Fig. 10. Under the embankment loads, the largest settlement occurs near the centerline of the foundation and upheaves on both sides. The upward displacement reaches a maximum approximately 36 m away from the foundation center. Compared with the GP composite and natural foundations, the total settlements of the PCP and LCP composite foundations are significantly smaller, which demonstrates that PCPs and LCPs can effectively reduce the total settlement of the foundation.

Fig. 11 shows the variations of the total settlements with time at the centerline under the embankment during construction and four years after construction. During the filling stage of the embankment, settlements increased nearly linearly with time. After the six-month waiting period, consolidation of the subsoil caused a large settlement. Rapid pavement construction quickly increased the foundation settlement. The total settlement after the completion of construction increased quickly initially, gradually slowed, and eventually reached stability. Compared with the rigid piles (e.g., PCPs and LCPs), GPs have a lower stiffness, thus causing a larger total settlement of the GP composite foundation, which is near the settlement of the natural foundation.

Fig. 12 shows the variations of the postconstruction settlements with time four years after construction. It can be seen that the postconstruction settlement of the PCP composite foundation is significantly smaller than the others. The numerical simulation results can be fit by a hyperbola

$$S_{pc} = -\frac{t - 278}{a + b(t - 278)} \tag{7}$$

where S_{pc} = postconstruction settlement; t = time; and a and b = regression parameters, where $1/a$ = instant rate of change in surface settlement when construction has been just completed, and $1/b$ = ultimate postconstruction settlement (S_{pcu}). Table 4 shows the parameters of the fitted curves.

Table 4 shows that, compared with other types of foundations, the PCP composite foundation has the smallest rate of change ($1/a$), which reflects that most of the pore pressure of the PCP composite foundation has dissipated during construction. It also has the largest b and thus the smallest ultimate postconstruction settlement ($S_{pcu} = 0.032$ m).

Although the total settlement of the PCP composite foundation is slightly larger than that of the LCP composite foundation, as shown in Fig. 12, the postconstruction settlement of the PCP composite foundation is much smaller than that of the LCP composite foundation. This is true because the PCP foundation has high strength, high

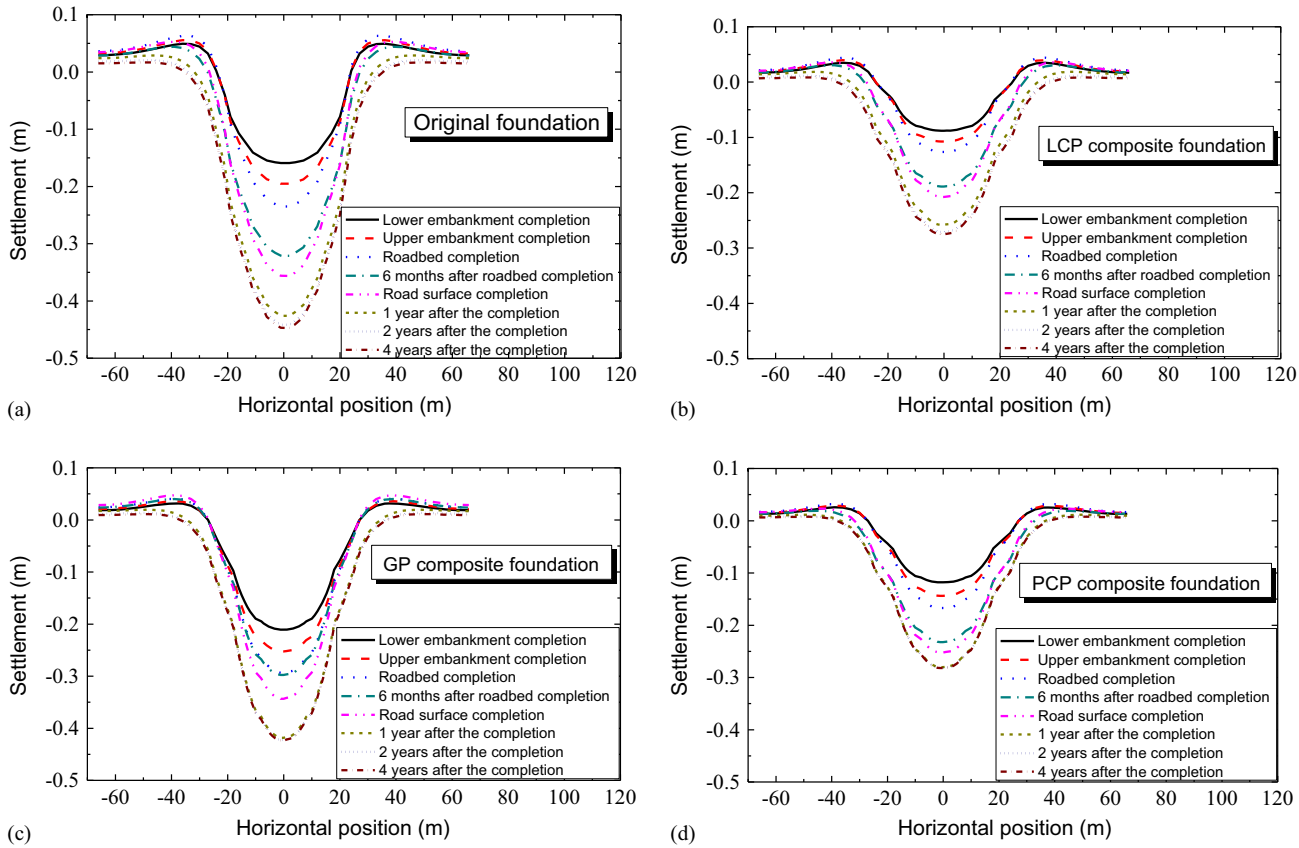

Fig. 10. Distribution curves of total ground surface settlement at different times: (a) original foundation; (b) LCP composite foundation; (c) GP composite foundation; (d) PCP composite foundation

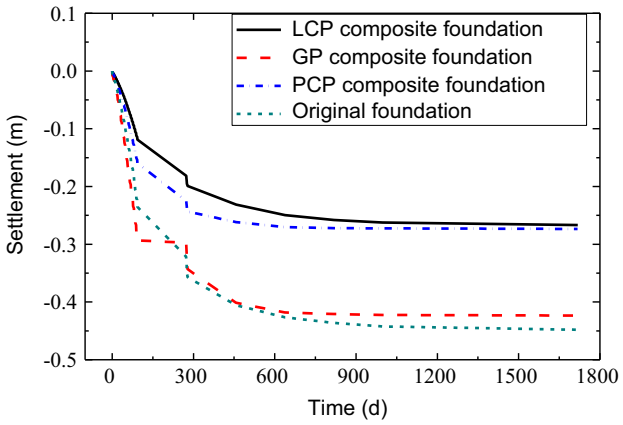

Fig. 11. Variations of total surface settlement with time at the centerline under the embankment

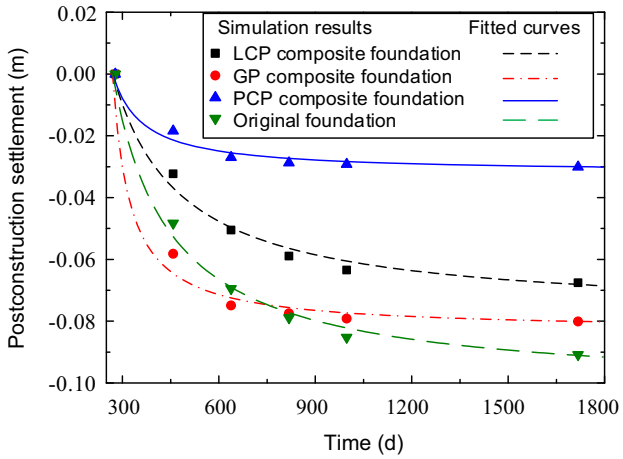

Fig. 12. Variations of postconstruction surface settlement with time

stiffness, and great permeability. As a result, the PCP foundation dissipates the excess pore-water pressure caused by the embankment load and accelerates subsoil consolidation during construction, thus decreasing postconstruction settlement. Compared with PCPs, GPs have a similar drainage performance but a higher postconstruction settlement (Fig. 13) due to higher excess pore pressure in the substratum, which requires a longer time to dissipate. This larger excess pore pressure is thus generated by a larger local stress that results from the uneven stress distribution in the substratum because GPs have a lower stiffness than PCPs.

Foundation Settlements at Different Depths

Fig. 13 shows the variations of the total foundation settlements with depth beneath the centerline of the embankment four years after construction. In the reinforced zone of the GP composite and natural foundations, the trends of the total settlements are similar; both show large settlements and decrease linearly with depth. The total settlements of the PCP and LCP composite foundations are similar and show a slight variation with depth. It is implied that the rigid piles (e.g., PCPs and LCPs) can work together with the soil in the

Table 4. Parameters of Fitted Curves

Types of foundation	a	b	S_{pcu} $(= 1/b)$ (m)
LCP composite foundation	2652.5	12.73	0.079
GP composite foundation	641.4	11.95	0.084
PCP composite foundation	2847.1	30.93	0.032
Original foundation	1716.4	9.71	0.103

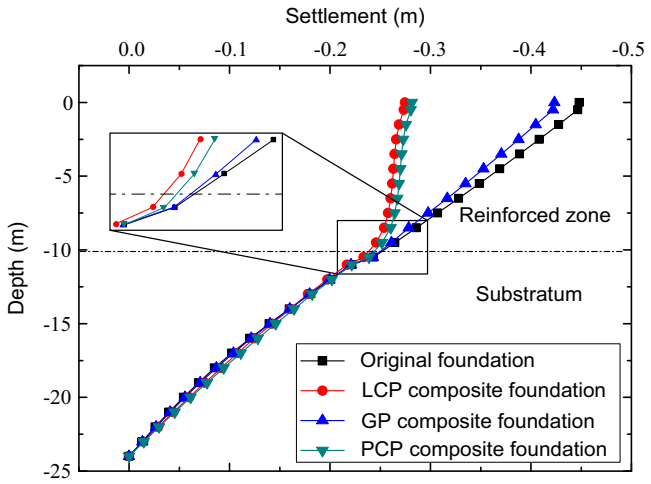

Fig. 13. Variations of foundation settlement with depth beneath the centerline of embankment four years after construction

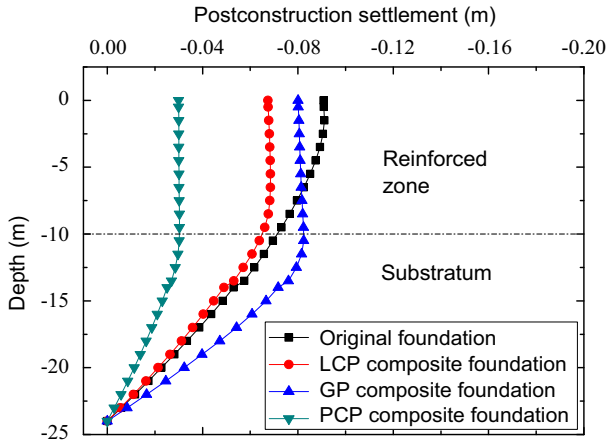

Fig. 14. Variations of postconstruction foundation settlement with depth beneath the centerline of embankment

reinforced area and prevent the subsoil from deforming vertically. In the substratum, for different foundations, the total settlements are similar; however, if the curves around the interface of the reinforced zone and substratum are amplified, differences between pile types can be found, as shown in Fig. 14. In the substratum, the total settlements of the rigid piles (e.g., LCPs and PCPs) are shown to be somewhat smaller than that of GPs. When different pile types are compared, it becomes apparent that the reinforced zones have different frictions with the soils, and thus, the loads born by the substratums are different. With high-stiffness piles such as LCPs and PCPs, the stress in the substratum will be smaller, thus resulting in a smaller settlement in the substratum.

Fig. 14 shows the variations of the postconstruction settlements with depth beneath the centerline of embankment. Postconstruction settlements vary significantly for the different foundations investigated. In the reinforced zone, the postconstruction settlements of all composite foundations show little variations with depth, which indicates little postconstruction vertical deformation. This implies that the postconstruction settlement of composite foundation surface is caused primarily by the deformation of substratum soil. For different piles, the influences of the substratum on the postconstruction settlements are significantly different. The postconstruction settlement of the PCP composite foundation is significantly smaller than those of the other foundations due to the high permeability of the piles, which forms a vertical drainage channel and allows the substratum to consolidate rapidly, reducing postconstruction settlement. Compared with PCPs, although GPs are also able to offer an improved vertical drainage channel, the lower strengths of these piles produce greater excess pore-water pressure during construction and so induce larger postconstruction settlements. Therefore, the PCP is a more effective method of improving soft ground than the LCP and GP.

Conclusions

In this study, a consolidation numerical model of a composite foundation was constructed based on the finite-difference method and Biot's consolidation theory. The excess pore pressure and settlement acquired from the numerical model are similar to the measured data from the in situ tests. Therefore, the numerical simulation method is reliable. The excess pore-water pressures, pile–soil stress ratios, lateral displacements, and settlements of different composite foundations under the loading of a road embankment were calculated. Comparisons between PCP, GP, and LCP composite foundations have been made. The primary conclusions are as follows:

1. The dissipation of excess pore-water pressure in the PCP composite foundation was quickest, which implies that PCP can significantly mitigate the development of excess pore-water pressure and thus effectively enhance the strength of subsoil.
2. The PCP composite foundation showed the lowest postconstruction settlement and lateral displacement, which proves that PCP can reduce the settlement of a foundation due to its high stiffness and permeability.

Therefore, having the high strength of a rigid pile and the large drainage ability of a granular pile, PCP is particularly suitable for reinforcing subsoils with low bearing capacities and poor water permeabilities.

Acknowledgments

This work was supported by the National Program on Key Basic Research Project of China (973 Program, 2015CB058101), the Science Fund for Distinguished Young Scholars of Shandong Province (JQ201416), the Natural Science Foundations of China (51479105, 51279094, 51308324, and 51379115), the Program for New Century Excellent Talents in Univ. of Ministry of Education of China (NCET-13-0340), the Fundamental Research Funds of Shandong Univ. (2014YQ013), and the Natural Science Foundations of Shandong Province of China (ZR2013EEQ025).

References

Ariyarathne, P., Liyanapathirana, D. S., and Leo, C. J. (2013). "Comparison of different two-dimensional idealizations for a geosynthetic-reinforced pile-supported embankment." *Int. J. Geomech.*, 10.1061/(ASCE)GM.1943-5622.0000266, 754–768.

Barron, R. A. (1948). "Consolidation of fine-grained soils by drain wells." *Trans. ASCE*, 113(1), 718–742.

Biot, M. A. (1956). "Theory of propagation of elastic waves in a fluid-saturated porous solid. I. Low-frequency range." *J. Acoust. Soc. Am.*, 28 (2), 168–178.
Biot, M. A. (1962). "Mechanics of deformation and acoustic propagation in porous media." *J. Appl. Phys.*, 33(4), 1482–1498.
Chen, L. Z., Liang, F. Y., Huang, D. Z., and Wang, G. C. (2004). "Field study on behavior of composite piled raft foundation for high-rise buildings." *Chin. J. Geotech. Eng.*, 26(2), 167–171 (in Chinese).
Conte, E., and Troncone, A. (2009). "Radial consolidation with vertical drains and general time-dependent loading." *Can. Geotech. J.*, 46(1), 25–36.
Cui, X. Z., Wang, C., and Zhou, Y. X. (2012). "Anti-earthquake mechanism of pervious concrete pile composite foundation." *J. Shandong Univ., Eng. Sci.*, 42(4), 86–91. (in Chinese).
Ferreira Pinto, A. P., and Delgado Rodrigues, J. (2008). "Stone consolidation: The role of treatment procedures." *J. Cult. Heritage*, 9(1), 38–53.
Ge, W., Zhang, J., Cao, D., Wang, B., and Pan, L. (2015). "Experimental study on the seismic behaviors of HRBF400 RC columns." *J. Test. Eval.*, 43(2), 353–262.
Guetif, Z., Bouassida, M., and Debats, J. M. (2007). "Improved soft clay characteristics due to stone column installation." *Comput. Geotech.*, 34 (2), 104–111.
Haldar, S., and Babu, G. (2010). "Failure mechanisms of pile foundations in liquefiable soil: Parametric study." *Int. J. Geomech.*, 10.1061/(ASCE) 1532-3641(2010)10:2(74), 74–84.
Hughes, J. M. O., and Withers, N. J. (1974). "Reinforcing of soft cohesive soils with stone columns." *Ground Eng.*, 7(3), 42–49.
Itasca Consulting Group. (2006). *Fast Lagrangian analysis of continua (FLAC) user's manual*, Itasca Consulting Group, Minneapolis.
Jia, J. Q., Wang, H. T., Li, J., Zhang X., and Fan, X. G. (2011). "Analysis of bearing capability of CFG pile composite foundation." *J. Chongqing Univ.*, 34(9), 117–127 (in Chinese).
Kevern, J. (2015). "Evaluating permeability and infiltration requirements for pervious concrete." *J. Test. Eval.*, 43(3), 554–564.
Lee, J. S., and Pande, G. N. (1998). "Analysis of stone-column reinforced foundations." *Int. J. Numer. Anal. Methods Geomech.*, 22(12), 1001–1020.
Le Hello, B., and Villard, P. (2009). "Embankments reinforced by piles and geosynthetics—Numerical and experimental studies with the transfer of load on the soil embankment." *Eng. Geol.*, 106(1–2), 78–91.
Leo, C. J. (2004). "Equal strain consolidation by vertical drains." *J. Geotech. Geoenviron. Eng.*, 10.1061/(ASCE)1090-0241(2004)130:3 (316), 316–327.
Luck, J. D., Workman, S. R., Higgins, S. F., and Coyne, M. S. (2006). "Hydrologic properties of pervious concrete." *Trans. ASAE*, 49(6), 1807–1813.
Majorana C., Mazzalai P., and Odorizzi S. (1983). "Prediction of the settlement of steel petroleum tanks resting on stone columns reinforced soil." *Proc., 8th European Conf. of Soils Mechanics and Foundations Engineering*, A. A. Balkema, Rotterdam, Netherlands, 271–274.
Montes, F., Valavala, S., and Haselbach, L. (2005). "A new test method for porosity measurements of portland cement pervious concrete." *J. ASTM Int.*, 2(1), 13.
MCPRC (Ministry of Construction of the People's Republic of China). (2002). "Technical code for ground treatment of buildings." *JGJ 79-2002*, Beijing.
MTPRC (Ministry of Transport of the People's Republic of China). (2004). "Specifications for design of highway subgrades." *JTG D30-2004*, Beijing.
MTPRC (Ministry of Transport of the People's Republic of China). (2006). "Technical specification for construction of highway subgrades." *JTG F10-2006*, Beijing.
Poorooshasb, H. B., and Meyerhof, G. G. (1997). "Analysis of behaviour of stone columns and lime columns." *Comput. Geotech.*, 20(1), 47–70.
Sariosseiri, F., and Muhunthan, B. (2009). "Effect of cement treatment on geotechnical properties of some Washington state soils." *Eng. Geol.*, 104(1–2), 119–125.
Schlüter, W., and Jefferies, C. (2002). "Modelling the outflow from a porous pavement." *Urban Water*, 4(3), 245–253.
Subba Rao, K., Allam, M., and Robinson, R. (2002). "An apparatus for evaluating adhesion between soils and solid surfaces." *J. Test. Eval.*, 30(1), 27–36.
Suleiman, M. T., Raich, A., and O'Loughlin, M. (2011). "Pervious concrete piles, an innovative ground improvement alternative." *Proc., 2011 NSF Engineering Research and Innovation Conf.*, Atlanta, Georgia.
Tennis, P. D., Leming, M. L., and Akers, D. J. (2004). *Pervious concrete pavements*, EB302, Portland Cement Association, Skokie, IL.
Terzaghi, K. (1925). "Principles of soil mechanics: I—Phenomena of cohesion of clays." *Eng. News-Rec.*, 95(19), 742–746.
Xie, K.-H., Lu, M.-M., Hu, A.-F., and Chen, G.-H. (2009). "A general theoretical solution for the consolidation of a composite foundation." *Comput. Geotech.*, 36(1–2), 24–30.
Yao, J., Wu, C., Liu, X., and Feng, K. (2015). "Effect of different interlayers of cement concrete pavements on vibration and anti-erosion of bases." *J. Test. Eval.*, 43(2), 434–442.
Yoshikuni, H. (1979). *Design and control of construction in the vertical drain method*, Gihoudou Publishing, Tokyo.
Zheng, J.-J., Abusharar, S. W., and Wang, X.-Z. (2008). "Three-dimensional nonlinear finite element modeling of composite foundation formed by CFG–lime piles." *Comput. Geotech.*, 35(4), 637–643.
Zhu, G., and Yin, J.-H. (2004). "Consolidation analysis of soil with vertical and horizontal drainage under ramp loading considering smear effects." *Geotext. Geomembr.*, 22(1–2), 63–74.